

Structural analysis of three extensional detachment faults with data from the 2000 Space-Shuttle Radar Topography Mission

Jon E. Spencer, Arizona Geological Survey, 416 W. Congress St. #100, Tucson, Arizona, 85701, USA; jon.spencer@azgs.az.gov

ABSTRACT

The Space-Shuttle Radar Topography Mission provided geologists with a detailed digital elevation model of most of Earth's land surface. This new database is used here for structural analysis of grooved surfaces interpreted to be the exhumed footwalls of three active or recently active extensional detachment faults. Exhumed fault footwalls, each with an areal extent of one hundred to several hundred square kilometers, make up much of Dayman dome in eastern Papua New Guinea, the western Gurla Mandhata massif in the central Himalaya, and the northern Tokorondo Mountains in central Sulawesi, Indonesia. Footwall curvature in profile varies from planar to slightly convex upward at Gurla Mandhata to strongly convex upward at northwestern Dayman dome. Fault curvature decreases away from the trace of the bounding detachment fault in western Dayman dome and in the Tokorondo massif, suggesting footwall flattening (reduction in curvature) following exhumation. Grooves of highly variable wavelength and amplitude reveal extension direction, although structural processes of groove genesis may be diverse.

INTRODUCTION

The February 2000 Shuttle Radar Topography Mission (SRTM) aboard the *Endeavour* acquired synthetic aperture radar data used to produce a new digital elevation model (DEM) of almost all Earth land areas between 60°N and 56°S latitude (Farr et al., 2007). The DEM is presently available for the entire survey area at 90 m spatial resolution (i.e., an elevation measurement is associated with each 90 m × 90 m area on Earth's surface). Heavily forested areas increase measured elevations because microwaves at the radar wavelengths are reflected by dense vegetation, and steep slopes produce local radar shadow zones with no data (Farr et al., 2007). Despite these problems, the new DEM provides very high-quality topographic data for 80% of Earth's land, much of which was not well surveyed before SRTM data acquisition and reduction.

The SRTM DEM is included in a global representation of bathymetry and topography maintained and upgraded by the Marine Geoscience Data System (MGDS) at Columbia University's Lamont-Doherty Earth Observatory. This global data set can be readily viewed online with the GeoMapApp[®] data visualization and analysis toolbox that is also available online from the MGDS at www.geomapp.org. This Java[™] application allows users to view topography and bathymetry at different

map scales, create cross sections, and save the images as graphics files. Elevations are represented by color, contours, and shaded relief, all of which are adjustable through the graphical user interface.

Domal, planar, and grooved surfaces, clearly visible in images derived from the SRTM DEM, are associated with some active or recently active low-angle normal faults. Some of these surfaces form remarkably smooth topography over tens to hundreds of square kilometers in regions otherwise deeply incised by rapid erosion. In this article, I present images of three of the most spectacular examples and evaluate some of the structural, tectonic, and geomorphic processes associated with inferred fault-footwall exhumation.

DAYMAN DOME, PAPUA NEW GUINEA

Dayman dome of the Suckling-Dayman massif in eastern Papua New Guinea is the westernmost metamorphic core complex in an east-west-trending belt that includes the D'Entrecasteaux Islands in the Solomon Sea (Fergusson, Goodenough, and Normanby Islands on Fig. 1A). Active extension is associated with westward propagation of the Woodlark spreading center (Fig. 1A; Martínez et al., 1999) following middle to late Tertiary accretion of a Paleogene island arc (Davies and Jaques, 1984; Davies and Warren, 1988). Subduction of the leading edge of the Australia–New Guinea passive continental margin beneath the island arc was followed by tectonic extension and exhumation of ca. 4 Ma eclogite and ca. 8 Ma coesite-eclogite in the D'Entrecasteaux Islands (Baldwin et al., 2004, 2008). These high-pressure and ultra-high-pressure metamorphic rocks are associated with domal and corrugated mylonitic shear zones and normal faults that are characteristic of core complexes (Davies and Warren, 1988; Hill et al., 1992; Little et al., 2007).

Most of Dayman dome consists of variably metamorphosed and deformed basaltic rocks and less-common limestone interpreted to be part of the subducted oceanic crust that was originally outboard of the early Cenozoic passive continental margin (Davies, 1980; Davies and Jaques, 1984). The extensional detachment fault (Mai'iu fault) at the north foot of Dayman dome is associated with greenschist-facies metamorphism in footwall rocks and a strong, tectonite fabric that is also domed (Davies, 1980). The tectonite fabric at the north foot of the dome is a lineated mylonitic shear zone with north-northeast-plunging lineations and normal displacement (Daczko et al., 2009). Mineral equilibria modeling suggests deformation at depths >20 km (Daczko et al., 2009). A 016° direction of extension is inferred from the average trend of 169 measured outcrop-scale lineations (Caffi, 2008), and is essentially parallel to the ~019° axis

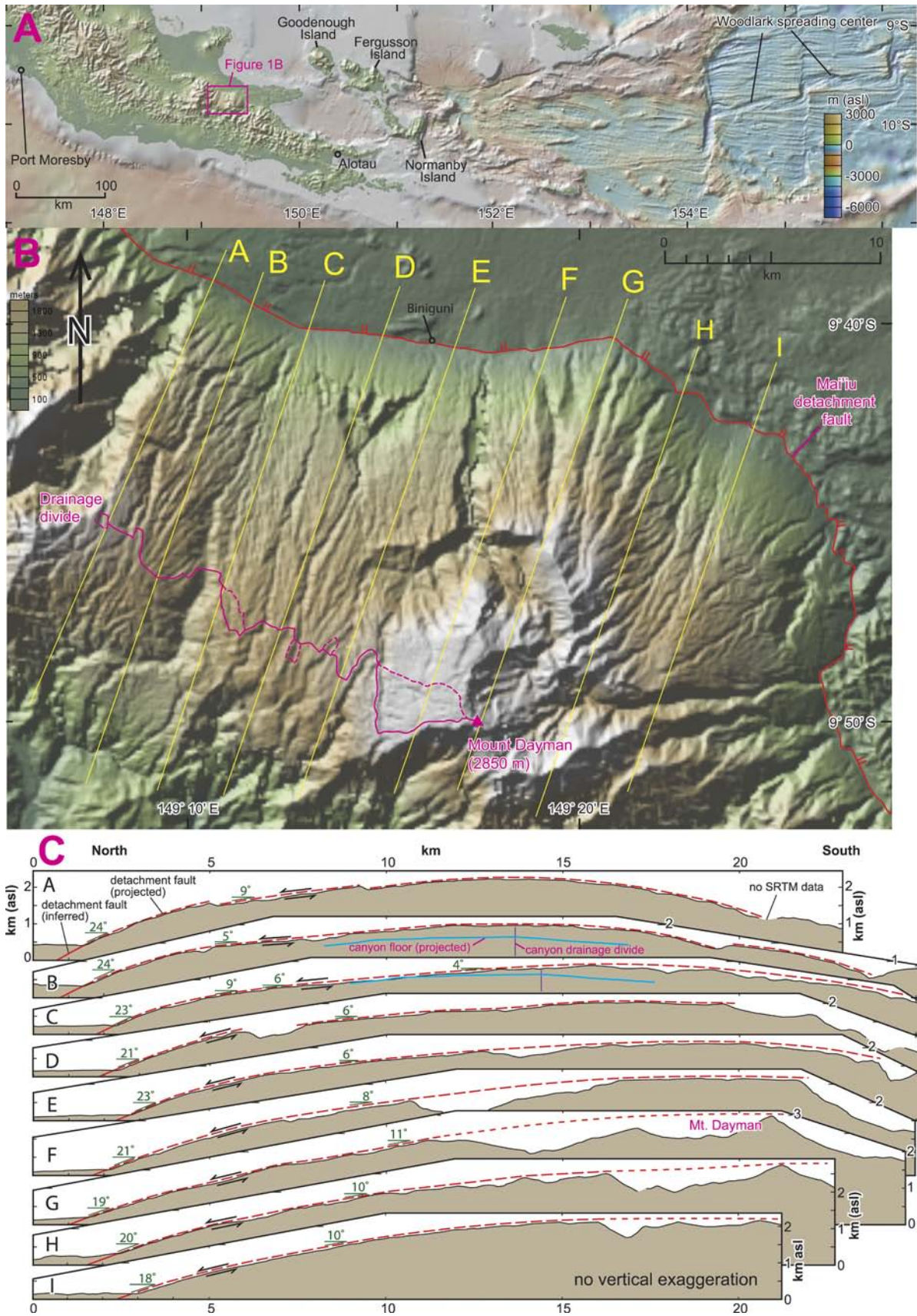


Figure 1. Elevation and shaded-relief maps and topographic cross sections derived from the Shuttle Radar Topography Mission (SRTM) digital elevation model using GeoMapApp[®]. (A) Map of Owen Stanley peninsula and D'Entrecasteaux Islands of easternmost Papua New Guinea, and Woodlark basin, with bathymetry derived from the Marine Geoscience Data System bathymetry database. (B) Map of Dayman dome (see Fig. 1A for location) showing trace of Mai'iu detachment fault (double ticks on hanging wall). Dashed lines are alternative locations for the drainage divide that are related to uncertainty in stream-flow paths at critical locations. (C) Topographic cross sections of Dayman dome (locations in B).

of the antiformal groove in northeastern Dayman dome (anti-form axis coincident with cross-section line G in Fig. 1B).

The smooth form of Dayman dome (Fig. 1B) is readily interpreted to be due to rapid and geologically recent tectonic exhumation from beneath an active normal fault (Ollier and Pain, 1980, 1981). Most drainages are highly linear and trend down the local slope of the dome. Six drainages in the northeastern part of the dome, located between cross-section lines G and I on Figure 1B, trend subparallel to the $\sim 019^\circ$ extension direction rather than locally down slope. The orientation of these drainages is plausibly due to a process by which stream channels in the hanging-wall block guide the lengthening streams as they are incised into the freshly denuded footwall (Spencer, 2000; Spencer and Ohara, 2008). This process is similar to the displacement-parallel elongation of stream channels that are cut and offset by strike-slip faults.

The fault ramp at the north foot of Dayman dome dips 18° to 24° in the direction of hanging-wall displacement (Fig. 1C). Western cross sections reveal greater fault dip at the foot of the dome (Fig. 1C) and greater curvature over the northern 5 km of the dome (Fig. 2, Dayman B and C vs. H and I). Greater curvature in western areas and flattening at higher elevations appear to be due to concave-downward bending during and/or immediately following tectonic exhumation, followed by unbending at higher elevations. Such behavior is consistent with the “rolling hinge” model for core-complex exhumation under conditions of low flexural strength (Wernicke and Axen, 1988; Buck, 1988) and may be the clearest example of such behavior in an active continental core complex.

A remarkable geomorphic feature revealed by SRTM data is a canyon, located between cross sections B and C in Figure 1B, that crosses the drainage divide at the crest of the antiformal western part of Dayman dome. South of the pass that divides the canyon, the stream bed plunges 4°S over 3 km, whereas north of the pass, the stream bed plunges 1.2°N over 4 km, at which point it steepens and enters its very slightly incised lower reach (Fig. 1C, cross sections B and C). The simplest explanation for the origin of this canyon is that uplift and arching of western Dayman dome split a previously incised, north-flowing stream in two, thus reversing the drainage direction of the now south-flowing part of the canyon (Spencer and Ohara, 2008). The abrupt 5° change in streambed plunge across the pass suggests that there has been some period of stability in the position of the drainage divide and that there has not been a recent transfer of an essentially horizontal reach of the northern stream channel to the southern stream channel. However, given ongoing uplift at the northern margin of the dome and the gentle 1.2° plunge of the upper stream bed north of the pass, transfer of a 4 km reach of the northern drainage to the southern drainage seems feasible if not likely in the geologic near future.

GURLA MANDHATA, HIMALAYA

The Gurla Mandhata massif is one of the larger gneiss domes along the backbone of the Himalayan orogen (e.g., Hodges, 2000; Fig. 3A). The massif is bounded to the west by the late Cenozoic Gurla Mandhata detachment fault that juxtaposes Tethyan Himalayan Paleozoic strata and Tertiary sedimentary rocks with footwall mylonitic schist, marble, granitoids, and

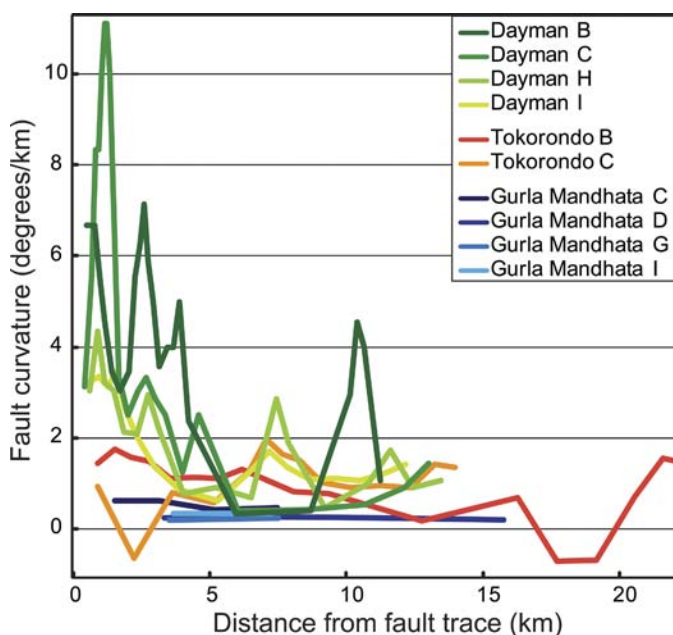


Figure 2. Fault curvature along selected displacement-parallel topographic profiles of three known or inferred detachment-fault footwalls. The spikes and troughs, especially apparent in the Dayman B cross section, result at least partly from differential erosion, where spikes represent subtle but developing ridges and troughs represent incipient stream valleys.

gneiss, with total offset estimated at $\sim 30\text{--}70$ km, directed toward 280° (Murphy et al., 2002). Detachment-fault displacement and extension have been interpreted as part of a dilational jog at the southeast end of the right-lateral Karakoram fault (Fig. 3A; Searle, 1996; Murphy et al., 2002).

A shaded relief map of the west side of the Gurla Mandhata massif (Fig. 3B) clearly reveals the extensive, generally westward-dipping fault ramp structurally below the detachment fault. A 4-km-long, 400-m-wide groove trending 284° is apparent in the detachment-fault ramp north of the town of Kejia (Figs. 3B and 3C). Groove depth decreases eastward from ~ 30 m in cross section J1 to ~ 8 m in cross section L1, beyond which the groove vanishes. Murphy et al. (2002, Figs. 2 and 7A therein) mapped a south-side-down normal fault approximately coincident with the groove. However, cross sections derived from SRTM data indicate that the groove is not simply a step in the fault ramp, but a smooth, two-sided furrow (Figs. 3B and 3C). Furthermore, examination of the Kejia groove with satellite imagery (using Google Earth) reveals numerous linear features that parallel the groove. I conclude that the Kejia groove and associated, more subtle grooves that are barely discernable on SRTM imagery (Figs. 3B and 3C) reflect the grooved form of the footwall ramp and that finer-scale lineation in color and landforms revealed by satellite imagery is likely due to parallel linear fabric elements within footwall tectonites (“mylonitic schist” of Murphy et al., 2002, Fig. 7A therein). Accordingly, the 284° trend of the Kejia groove is used here to indicate detachment-fault displacement direction, which is nearly identical to the $280^\circ \pm 4^\circ$ trend of stretching lineations measured in footwall mylonites of the Gurla Mandhata massif by Murphy et al. (2002).

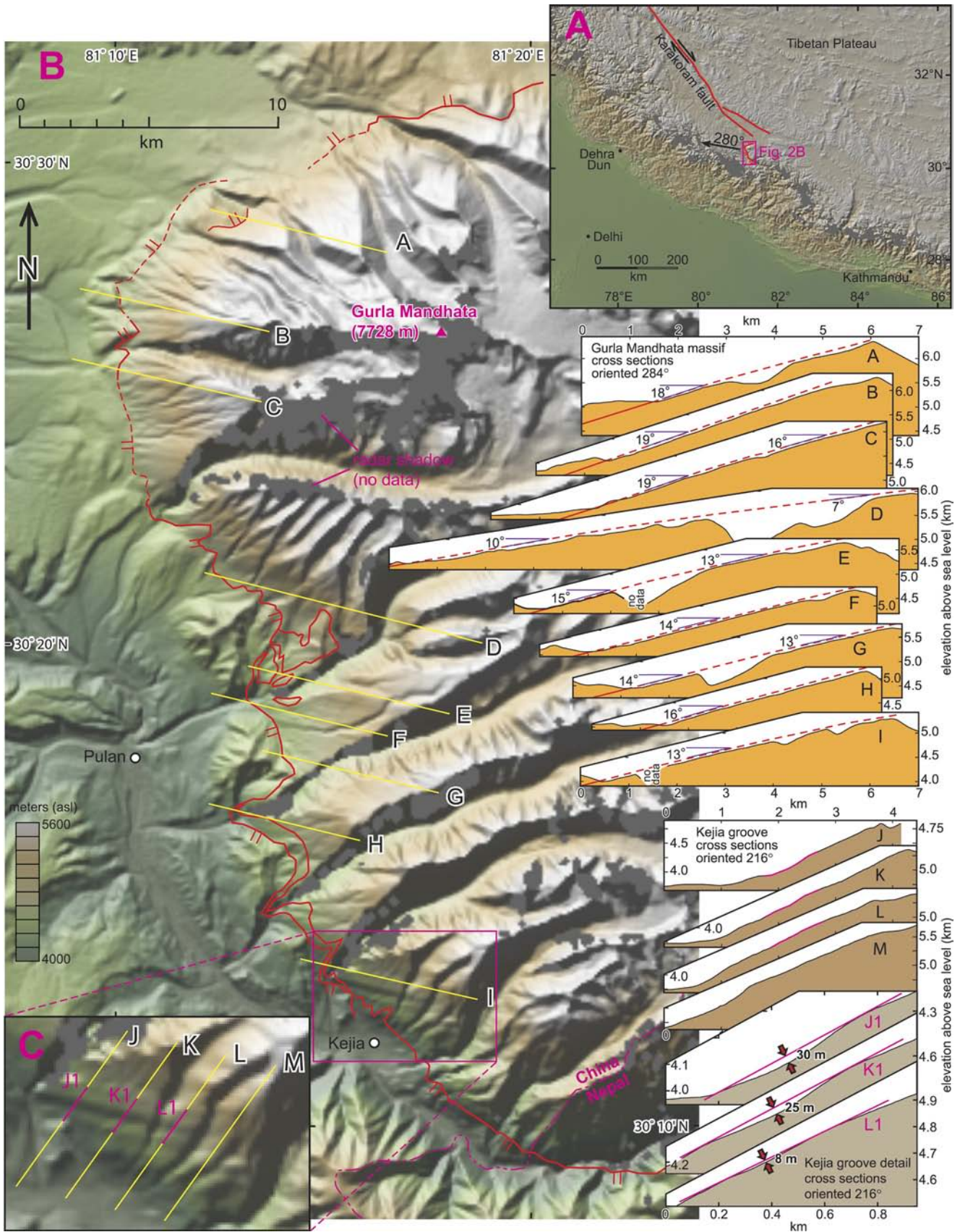


Figure 3. Elevation and shaded-relief maps and topographic cross sections derived from the Shuttle Radar Topography Mission digital elevation model using GeoMapApp[®]. (A) Map of the central Himalaya and southwestern Tibetan plateau. (B) Map of the west side of the Gurla Mandhata massif (location in A) and topographic cross sections (no vertical exaggeration). Faults (red lines, double ticks on detachment-fault hanging wall) from Murphy et al. (2002). (C) Close-up map of Kejia groove showing location of cross sections. Note that the 216° trend of the cross sections is not perpendicular to the 280° trend of the Kejia groove, but was chosen because it avoids intervening drainages that would obscure the cross-sectional representation of the groove.

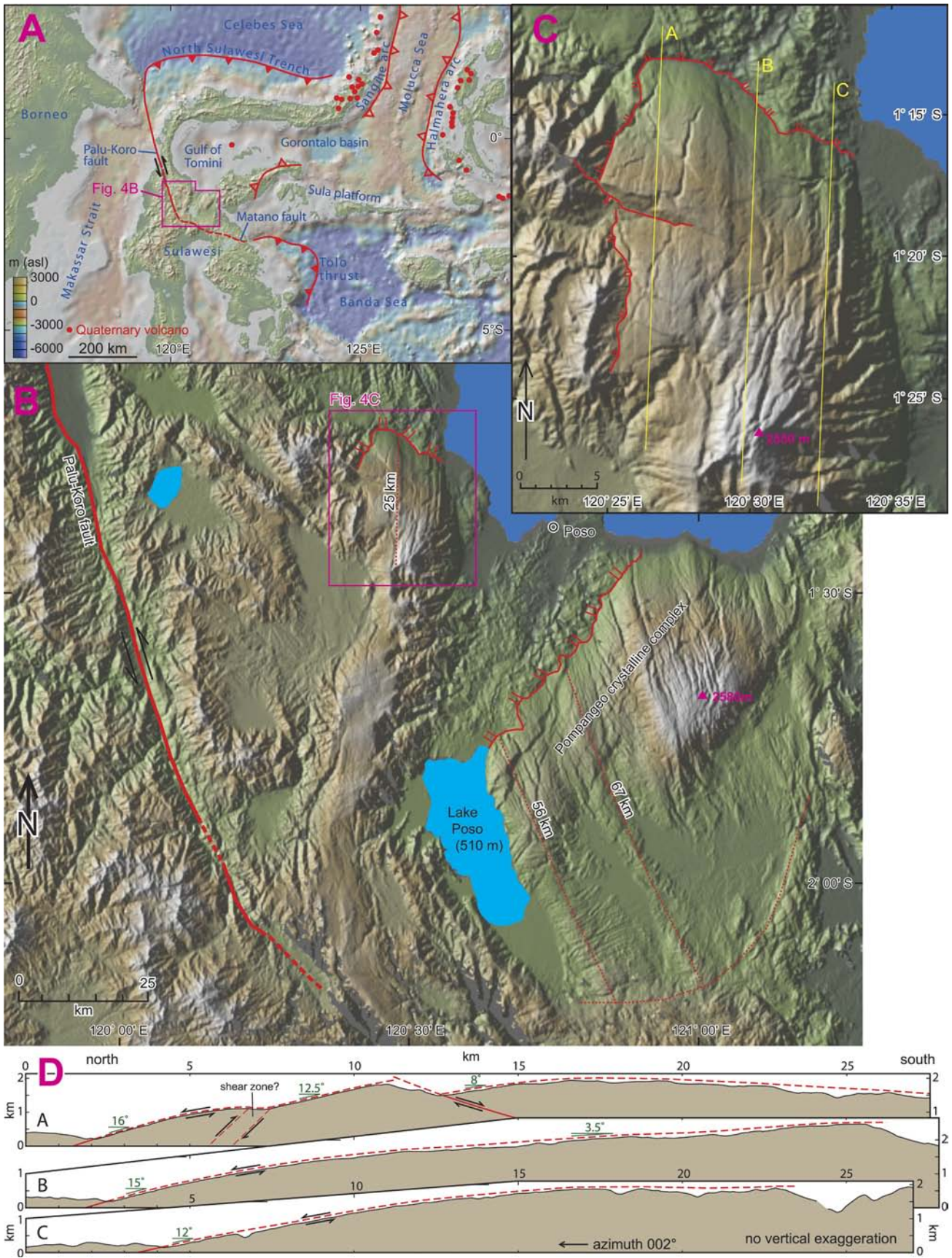


Figure 4. Elevation and shaded-relief maps and topographic cross sections derived from the SRTM DEM using GeoMapApp®. (A) Map of the Sulawesi and surrounding areas, with bathymetry derived from the Marine Geoscience Data System bathymetry database. Geologic features from Hamilton (1979) and Silver et al. (1983). (B) Map of central Sulawesi (location in A) showing inferred detachment faults (double ticks on hanging wall) and high-angle faults (red lines). (C) Map of the Tokorondo massif (location in B) showing inferred detachment fault and high-angle faults. (D) Topographic cross sections (location in C) of Tokorondo massif.

Nine topographic profiles of the detachment-fault footwall ramp on the west side of the Gurla Mandhata massif, all oriented parallel to the 284° trend of the Kejia groove and inferred fault-displacement direction (Fig. 3, cross sections A–I), reveal the low-curvature cross-sectional form of the fault ramp in this profile orientation. The component of fault dip (i.e., apparent dip) in the extension direction along profile D (Fig. 3), which is the longest cross section, changes only ~3° over 11 km. This contrasts with Dayman dome, where much higher curvature could reflect lower flexural strength in footwall rocks during tectonic exhumation (Fig. 2).

Also apparent in cross sections A–I is variation among cross sections in extension-parallel fault dip. The fault ramp in the area directly west of Gurla Mandhata dips 18°–19° in the 284° direction (cross sections A–C), whereas to the south, within a synformal megagroove in the detachment fault, groove-parallel fault dip is 10° or less (cross section D). If map-view extension direction is consistently parallel to the Kejia groove along the west flank of the massif (or to some other extension vector), then uplift paths of different parts of the footwall must be different, with the area west of Gurla Mandhata ascending more steeply than areas to the south. Such behavior would result in an increase in the surface area of the detachment fault over time. Alternatively, map-view extension direction varies across the massif, perhaps with footwall displacement vectors converging slightly toward antiforms, such as Gurla Mandhata, and away from flanking, lower-lying areas. Either possibility might have observable consequences in footwall rocks. For example, convergent flow of footwall rocks toward Gurla Mandhata should have produced slightly radial lineations.

TOKORONDO MASSIF, SULAWESI, INDONESIA

The active tectonics of eastern Indonesia are among the most complex on Earth. The region is a plate-tectonic triple junction that accommodates convergence between the Pacific, Eurasian, and Indo-Australian plates, but in detail, the area is characterized by such features as colliding arcs and rotating microplates (e.g., Hamilton, 1979; Hall, 2002, 2008). Northward displacement of northern Sulawesi over the Celebes Sea floor along a geologically young subduction zone has not yet been sufficient to initiate arc magmatism (Fig. 4A; Silver et al., 1983). The Palu-Koro left-lateral fault is linked to the North Sulawesi trench and accommodates northward movement of northern Sulawesi relative to the more stable interior of western Indonesia (Bellier et al., 2001). Features identified as extensional detachment faults in central Sulawesi are located east of the Palu-Koro fault and may be kinematically linked to it.

The topography of central Sulawesi as revealed by SRTM data is characterized by two large, corrugated landforms that are readily interpreted as the denuded footwalls of extensional detachment faults (Fig. 4B). Both domal landforms are corrugated on a scale of kilometers and both are bounded to the north by an abrupt transition to a region of completely different topographic character. The northern transitions are readily interpreted as gently north-dipping detachment faults.

The larger, southeastern corrugated landform, centered on the Pompangeo Mountains and extending over ~2000 km², consists primarily of marble, phyllite, quartz-mica schist, and metaconglomerate (Parkinson, 1998). Stretching lineations

($n = 19$) within strong transposition foliation approximately parallel the linear landforms (Parkinson, 1998, Fig. 5 therein). Both Hamilton (1979) and Parkinson (1998) attributed the lineated geomorphology to thrust imbrication, with thrusts striking parallel to the ridges. On the basis of geomorphologic similarity to Dayman dome, Spencer and Ohara (2008) interpreted the Pompangeo crystalline complex as the exhumed footwall of a detachment fault and suggested that the stretching lineations identified by Parkinson (1998) are products of mylonitic shearing during core-complex exhumation. The corrugated form of the crystalline complex extends southward to areas that were also possibly exhumed from below the detachment fault, suggesting as much as 60 to 70 km of extension (Fig. 4B).

The smaller corrugated massif, located west of Poso in the northern Tokorondo Mountains (Fig. 4B), is a lineated, elongate, gently north-plunging half-dome with a remarkably smooth surface covering ~300 km² (Fig. 4C). The sharp northern and western boundaries of the massif are interpreted to be a detachment fault (Fig. 4C). Three parallel grooves on the eastern side of the Tokorondo massif, spaced ~1 km apart and with crest-to-trough amplitude of a few tens of meters, extend along a 002° trend for ~12 km. These grooves, and more subtle grooves farther west on the massif (Fig. 4C), are interpreted as primary grooves in the detachment-fault footwall that reveal displacement direction. The small wavelength of the Tokorondo grooves, combined with their significant length, is characteristic of grooves on deep-sea rather than continental core complexes (e.g., Ohara et al., 2001). The groove-parallel extent of inferred footwall exhumation is at least 24 km (Fig. 4D, cross section B), indicating at least this amount of extension. In cross section (Fig. 4D), the overall curvature of the denuded fault footwall is intermediate between Dayman dome and Gurla Mandhata (Fig. 2), suggesting moderate flexural strength during exhumation. Decreasing curvature with distance from the northern edge of the exhumed footwall suggests flattening following exhumation (Figs. 2 and 4D, cross section B).

Two studies have concluded that central and northern Sulawesi are rotating clockwise about a point near the eastern end of the north arm of Sulawesi, with the Matano and Palu-Koro faults forming a small-circle transform boundary of the rotating block (Silver et al., 1983; Bellier et al., 2006; see also Soquet et al., 2006). However, analysis presented here of SRTM-derived images of central Sulawesi reveals what appear to be two large detachment faults that have potentially accommodated up to 100 km of north-south extension between northern and central Sulawesi. If interpreted correctly, the detachment faults indicate the need for a reappraisal of Plio-Quaternary kinematic models for the Sulawesi region.

CONCLUSIONS

Greater footwall curvature (in extension-parallel cross sections) and footwall flattening with displacement away from the flanking detachment fault, as are apparent at Dayman dome and in the central part of the Tokorondo massif (Fig. 4D, cross section B), suggest low bending strength, perhaps due to elevated geothermal gradients during subaerial exhumation. Footwall grooves are not obviously related to footwall curvature, however, as might be expected if groove genesis

was associated with elevated footwall temperature and greater pliability. Furthermore, it is not known if the Tokorondo grooves were shaped by plastic processes while the Kejia groove was shaped by brittle processes, or if footwall composition (e.g., carbonate vs. quartzite) is important in groove genesis. It is clear, however, that SRTM data have provided geologists with a wealth of geomorphic information with which to investigate regions of active extensional tectonics and to outline issues for future field-based structural and thermochronologic investigations.

ACKNOWLEDGMENTS

I thank Nathan Daczko (Macquarie University) for generously sharing results from his 2006 geologic expedition to Dayman dome. I also thank Paul Kapp and an anonymous reviewer for constructive reviews.

REFERENCES CITED

- Baldwin, S.L., Monteleone, B., Webb, L.E., Fitzgerald, P.G., Grove, M., and Hill, E.J., 2004, Pliocene eclogite exhumation at plate tectonic rates in eastern Papua New Guinea: *Nature*, v. 431, p. 263–267.
- Baldwin, S.L., Webb, L.E., and Monteleone, B.D., 2008, Late Miocene coesite-eclogite exhumed in the Woodlark Rift: *Geology*, v. 36, p. 735–738; doi: 10.1130/G25144A.1.
- Bellier, O., Sébrier, M., Beaudouin, T., Villeneuve, M., Braucher, R., Bourlès, D., Siame, L., Putranto, E., and Pratomo, I., 2001, High slip rate for a low seismicity along the Palu-Koro active fault in central Sulawesi (Indonesia): *Terra Nova*, v. 13, p. 463–470.
- Bellier, O., Sébrier, M., Seward, D., Beaudouin, T., and Villeneuve, M., 2006, Fission track and fault kinematics analyses for new insight into the late Cenozoic tectonic regime changes in west-central Sulawesi (Indonesia): *Tectonophysics*, v. 413, p. 201–220.
- Buck, W.R., 1988, Flexural rotation of normal faults: *Tectonics*, v. 7, p. 959–973.
- Caffi, P., 2008, Evolution of an active metamorphic core complex, Suckling-Dayman Massif, eastern PNG [B.S. honours thesis]: Macquarie University, Sydney, Australia, 165 p.
- Daczko, N.R., Caffi, P., Halpin, J.A., and Mann, P., 2009, Exhumation of the Dayman dome metamorphic core complex, eastern Papua New Guinea: *Journal of Metamorphic Geology*, v. 27, p. 405–422; doi: 10.1111/j.1525-1314.2009.00825.x.
- Davies, H.L., 1980, Folded thrust fault and associated metamorphics in the Suckling-Dayman massif, Papua New Guinea: *American Journal of Science*, v. 280-A, p. 171–191.
- Davies, H.L., and Jaques, A.L., 1984, Emplacement of ophiolite in Papua New Guinea: Geological Society, London, Special Publication 13, p. 341–350; doi: 10.1144/GSL.SP.1984.013.01.27.
- Davies, H.L., and Warren, R.G., 1988, Origin of eclogite-bearing, domed, layered metamorphic complexes (“core complexes”) in the D’Entrecasteaux Islands, Papua New Guinea: *Tectonics*, v. 7, p. 1–21.
- Farr, T.G., Rosen, P.A., Caro, E., Crippen, R., Duren, R., Hensley, S., Kobrick, M., Paller, M., Rodriguez, E., Roth, L., Seal, D., Shaffer, S., Shimada, J., Umland, J., Werner, M., Oskin, M., Burbank, D., and Alsdorf, D., 2007, The Shuttle Radar Topography Mission: *Reviews of Geophysics*, v. 45, RG2004; doi: 10.1029/2005RG000183.
- Hall, R., 2002, Cenozoic geological and plate tectonic evolution of SE Asia and the SW Pacific: computer-based reconstructions, model and animations: *Journal of Asian Earth Sciences*, v. 20, p. 353–434.
- Hall, R., 2008, Continental growth at the Indonesian margins of southeast Asia, in Spencer, J.E., and Tittley, S.R., eds., *Ores and orogenesis: Circum-Pacific tectonics, geologic evolution, and ore deposits: Arizona Geological Society Digest 22*, p. 245–258.
- Hamilton, W., 1979, *Tectonics of the Indonesia region: U.S. Geological Survey Professional Paper 1078*, 345 p., with tectonic map of Indonesia, scale 1:5,000,000.
- Hill, E.J., Baldwin, S.L., and Lister, G.S., 1992, Unroofing of active metamorphic core complexes in the D’Entrecasteaux Islands, Papua New Guinea: *Geology*, v. 20, p. 907–910.
- Hodges, K.V., 2000, Tectonics of the Himalaya and southern Tibet from two perspectives: *Geological Society of America Bulletin*, v. 112, p. 324–350.
- Little, T.A., Baldwin, S.L., Fitzgerald, P.G., and Monteleone, B., 2007, Continental rifting and metamorphic core complex formation ahead of the Woodlark spreading ridge, D’Entrecasteaux Islands, Papua New Guinea: *Tectonics*, v. 26, doi: 10.1029/2005TC001911.
- Martínez, F., Taylor, B., and Goodliffe, A.M., 1999, Contrasting styles of seafloor spreading in the Woodlark Basin: Indications of rift-induced secondary mantle convection: *Journal of Geophysical Research*, v. 104, p. 12,909–12,926.
- Murphy, M.A., Yin, A., Kapp, P., Harrison, T.M., Manning, C.E., and Ryerson, F.J., 2002, Structural evolution of the Gurla Mandhata detachment system, southwest Tibet: Implications for the eastward extent of the Karakoram fault system: *Geological Society of America Bulletin*, v. 114, p. 428–447.
- Ohara, Y., Yoshida, T., Kato, Y., and Kasuga, S., 2001, Giant megamullion in the Parece Vela backarc basin: *Marine Geophysical Research*, v. 22, p. 47–61.
- Ollier, C.D., and Pain, C.F., 1980, Actively rising surficial gneiss domes in Papua New Guinea: *Journal of the Geological Society of Australia*, v. 27, p. 33–44.
- Ollier, C.D., and Pain, C.F., 1981, Active gneiss domes in Papua New Guinea—new tectonic landforms: *Zeitschrift für Geomorphologie*, v. 25, no. 2, p. 133–145.
- Parkinson, C., 1998, An outline of the petrology, structure and age of the Pompangeo Schist Complex of central Sulawesi, Indonesia: *The Island Arc*, v. 7, no. 1-2, p. 231–245.
- Searle, M., 1996, Geological evidence against large-scale pre-Holocene offsets along the Karakoram fault: Implications for the limited extrusion of the Tibetan Plateau: *Tectonics*, v. 15, p. 171–186.
- Silver, E.A., McCaffrey, R., and Smith, R.B., 1983, Collision, rotation, and the initiation of subduction in the evolution of Sulawesi, Indonesia: *Journal of Geophysical Research*, v. 88, p. 9407–9418.
- Socquet, A., Simons, W., Vigny, C., McCaffrey, R., Subarya, C., Sarsito, D., Ambrosius, B., and Spakman, W., 2006, Microblock rotations and fault coupling in SE Asia triple junction (Sulawesi, Indonesia) from GPS and earthquake slip vector data: *Journal of Geophysical Research*, v. 111, 15 p., B08409; doi: 10.1029/2005JB003963.
- Spencer, J.E., 2000, Possible origin and significance of extension-parallel drainages in Arizona’s metamorphic core complexes: *Geological Society of America Bulletin*, v. 112, p. 727–735.
- Spencer, J.E., and Ohara, Y., 2008, Magmatic and tectonic continuous casting in the circum-Pacific region, in Spencer, J.E., and Tittley, S.R., eds., *Ores and orogenesis: Circum-Pacific tectonics, geologic evolution, and ore deposits: Arizona Geological Society Digest 22*, p. 31–53.
- Wernicke, B., and Axen, G.J., 1988, On the role of isostasy in the evolution of normal fault systems: *Geology*, v. 16, p. 848–851.

Manuscript received 20 May 2009; accepted 17 Jan. 2010. 